

Citation for published version:

Sharpless, CM, Aeschbacher, M, Page, SE, Wenk, J, Sander, M & McNeill, K 2014, 'Photooxidation-induced changes in optical, electrochemical, and photochemical properties of humic substances', *Environmental Science and Technology*, vol. 48, no. 5, pp. 2688-2696. <https://doi.org/10.1021/es403925g>

DOI:

[10.1021/es403925g](https://doi.org/10.1021/es403925g)

Publication date:

2014

Document Version

Early version, also known as pre-print

[Link to publication](#)

This is the author's submitted version of an article published by the American Chemical Society, and available in final published form at: Sharpless, CM, Aeschbacher, M, Page, SE, Wenk, J, Sander, M & McNeill, K 2014, 'Photooxidation-induced changes in optical, electrochemical, and photochemical properties of humic substances' *Environmental Science and Technology*, vol 48, no. 5, pp. 2688-2696., [10.1021/es403925g](https://doi.org/10.1021/es403925g)

University of Bath

Alternative formats

If you require this document in an alternative format, please contact:
openaccess@bath.ac.uk

General rights

Copyright and moral rights for the publications made accessible in the public portal are retained by the authors and/or other copyright owners and it is a condition of accessing publications that users recognise and abide by the legal requirements associated with these rights.

Take down policy

If you believe that this document breaches copyright please contact us providing details, and we will remove access to the work immediately and investigate your claim.

**Photooxidation-Induced Changes in Optical, Electrochemical and Photochemical
Properties of Humic Substances**

Authors

Charles M. Sharpless^{a,*}; Michael Aeschbacher^{b,c}; Sarah E. Page^c; Jannis Wenk^{c,d,e,f}; Michael
Sander^c; Kristopher McNeill^c

Affiliations

^a Department of Chemistry, University of Mary Washington, USA-22401 Fredericksburg, VA

^b BMG Engineering AG, CH-8952 Schlieren, Switzerland

^c Institute of Biogeochemistry and Pollutant Dynamics, ETH Zurich, CH-8092 Zürich,
Switzerland

^d Eawag, Swiss Federal Institute of Aquatic Science and Technology, CH-8600 Dübendorf,
Switzerland

^e Department of Civil & Environmental Engineering, University of California at
Berkeley, Berkeley, CA 94720, USA

^f ReNUWIt Engineering Research Center

* Corresponding author

E-mail: csharp@umw.edu

Phone: +001 540.654.1405

Fax: +001 540.654.1081

Number of pages: 31, with references and figures
Number of figures: six: five under 3.3” limit (est. 1500 words) one large (est. 600 words)
Number of tables: none
Number of words: 4,685 in main MS; estimate as 6,785 with figures

Abstract

Three dissolved humic substances (HS), two aquatic fulvic acids and one soil humic acid were irradiated to examine the resulting changes in HS redox and photochemical properties, the relationship between these changes, and their relationship to changes in the optical properties. For all HS, irradiation caused photooxidation as shown by decreasing electron donating capacities. This was accompanied by decreases in specific UV absorbance and increases in the E2/E3 ratio (254 nm absorbance divided by 365 nm). In contrast, photooxidation had little effect on the samples' electron accepting capacities. The coupled changes in optical and redox properties for the different HS suggest that phenols are an important determinant of aquatic HS optical properties and that quinones may play a more important role in soil HS. Apparent quantum yields of H_2O_2 , $\cdot\text{OH}$, and triplet HS decreased with photooxidation, thus demonstrating selective destruction of HS photosensitizing chromophores. In contrast, singlet oxygen ($^1\text{O}_2$) quantum yields increased, which is ascribed to either decreased $^1\text{O}_2$ quenching within the HS microenvironment or the presence of a pool of photostable sensitizers. The photochemical properties show clear trends with SUVA and E2/E3, but the trends differ substantially between aquatic and soil HS. Importantly, photooxidation produces a relationship between the $^1\text{O}_2$ quantum yield and E2/E3 that differs distinctly from that observed with untreated HS. This suggests that there may be watershed-specific correlations between HS chemical and optical properties that reflect the dominant processes controlling the HS character.

Introduction

Dissolved organic matter (DOM) is a ubiquitous component of natural surface waters produced by transformation of plant and plankton-derived precursor molecules. It comprises

moderately hydrophobic aromatic polyelectrolytes of variable molecular weight (100's to 1000's of g/mol) (1,2) and plays an important role in the biogeochemistry of aquatic environments. For example, microorganisms use DOM as a source of C and N and as an electron shuttle in anaerobic respiration (3). DOM also plays important roles in pollutant dynamics, for instance by sorbing organic contaminants and chelating trace and heavy metals (4,5). Absorption of sunlight by aromatic chromophores in DOM (1,6) leads to formation of reactive oxygen species (ROS) including singlet oxygen ($^1\text{O}_2$), hydrogen peroxide (H_2O_2), and hydroxyl radical ($\bullet\text{OH}$) (7,8). DOM triplet states ($^3\text{DOM}^*$) are both important precursor species for many of these ROS and strong oxidants in DOM-sensitized photoreactions (7-9). Together, these photooxidants play a critical role in the redox speciation of trace metals (10-12), transformation rates of organic contaminants (9,13-15), and solar inactivation of pathogens (16).

Absorption of sunlight also leads to DOM photobleaching (destruction of chromophores), photooxidation, and production of low molecular weight organic compounds and inorganic species such as CO and CO_2 (17-23). These processes may involve the loss of specific functional moieties and lead to changes in the physicochemical and optical properties of DOM. For example, lignin phenols disappear rapidly in the early stages of photooxidation (24-26). Other studies have used FT-ICR-MS and ^{13}C NMR spectroscopy to show that DOM loses aromatic groups during photooxidation (27,28). Concomitant changes in DOM optical properties are consistent with a loss of DOM aromaticity (% aromatic C by ^{13}C NMR), including decreases in specific UV absorbance (SUVA, absorbance per mg-C) and fluorescence intensity, and increases in spectral slope and the E2/E3 ratio (ratio of the absorbance at 254 to 365 nm) (29-35).

The influence of photooxidation on DOM photochemistry remains poorly investigated and understood. Substantial effects seem plausible given that photooxidation changes E2/E3 and SUVA values and that these parameters correlate with quantum yields of $^1\text{O}_2$ and CO photoproduction (36-41). Zhang *et al.* reported that prolonged irradiation decreased quantum yields for CO production (38). To our knowledge, however, no systematic study exists of how irradiation affects photooxidant quantum yields. Cavani *et al.* reported that $^1\text{O}_2$ production rates from peat humic acid were unaffected by eight hours of irradiation at 365 nm (42). In contrast, Andrews *et al.* reported that H_2O_2 quantum yields for various aquatic samples decreased with increasing irradiation using simulated sunlight (43). The results of these two studies are, however, difficult to compare since they not only involve different ROS but also used different samples, methods, irradiation times, and assessment endpoints (i.e., production rates versus quantum yields). Furthermore, the observed trends were not related to the extent of DOM oxidation, which was, until recently, difficult to quantify due to the lack of an appropriate method. The introduction of mediated electrochemical oxidation and reduction (MER and MEO, respectively) now allows reliable quantification of DOM redox state in terms of electron donating and accepting capacities (EDC and EAC) (44,45). The EDC and EAC of DOM have been ascribed to phenol and quinone moieties, respectively, which are also chromophores believed to play an important role in DOM photochemistry (8,9,46-49).

The objective of this study was to systematically investigate the effects of photooxidation on DOM optical, electrochemical and photochemical properties. Studying these changes simultaneously is expected to provide insights into relationships between DOM aromaticity, redox-state, and photoreactivity and to improve understanding of the DOM photobleaching process. Experiments were conducted with three dissolved humic substances (HS): two aquatic

fulvic acids (FAs) and, for contrast, a soil humic acid (HA). Changes in the absorption spectra and apparent quantum yields for the photooxidants $^1\text{O}_2$, H_2O_2 , $\cdot\text{OH}$, and triplet HS ($^3\text{HS}^*$) were measured as a function of irradiation time. The extent of photooxidation was quantified by monitoring changes in EDC and EAC. Spectroscopic data were also used to examine whether correlations between optical and photochemical properties for photooxidized HS are consistent with reported correlations for native DOM isolates (36,37).

Materials & Methods

Materials. Nordic Aquatic Fulvic Acid (NAFA), Suwannee River Fulvic Acid (SRFA), and Elliot Soil Humic Acid (ESHA) standards were obtained from the International Humic Substances Society (IHSS, www.humicsubstances.org) and used as received. Details for other materials can be found in the *Supporting Information*.

Solutions for Irradiation. All solutions were prepared with Nanopure water (Barnstead) with resistivity $>18.2 \text{ M}\Omega \text{ cm}$. The photooxidation experiments were conducted at high HS concentrations (250 mg/L) to ensure the availability of sufficient HS for subsequent analyses. The solutions were prepared by dissolving 25 mg of solid HS isolate in 50 mL of H_2O followed by addition of 1 M NaOH to adjust the pH to 8.0. After pH stabilization ($> 30 \text{ min}$), solutions were stirred overnight at room temperature and subsequently diluted to a total volume of 100 mL. The pH was readjusted to 7.0, followed by filtration (0.22 μm) to remove particulate material and sterilize the samples, which were stored for six days at 4 $^\circ\text{C}$ before use in experiments.

Irradiation Procedure. Aliquots of each HS solution (20 to 25 mL) were transferred to 18 mm diameter quartz tubes containing a magnetic stir bar. The tubes were capped with septa

fitted to allow air sparging of the solutions during irradiation. Sample tubes were placed below the lamp at approximately 30° from horizontal and immersed in a recirculating water bath at 25 °C. A Suntest solar simulator was used at a nominal setting of 700 W m⁻². The total photon flux (300 to 700 nm) was 1.4x10⁻⁴ Es L⁻¹ s⁻¹, as estimated from *p*-nitroanisole/pyridine actinometry (50). Samples were irradiated for a total of 59 h in periods of 11 or 12 h with continuous stirring and sparging with synthetic air. The air bubbles were confined to the center of the sparged solutions and, because the solutions were optically thick, likely had minimal effect on the radiation delivery.

Solution volumes (determined gravimetrically) and pH were measured at the beginning and end of each irradiation period. After each period, small amounts of water were added to replace evaporative losses (always < 0.2 mL) and small volumes of 1 M NaOH were added to re-adjust the pH to 7.0 (the pH never fell below 6.5). At selected intervals, aliquots of solution were removed for analysis and experimentation. To allow for intra-HS redox equilibration, these were stored at 4 °C for at least 3 d before conducting electrochemical and photochemical experiments. All experiments and analyses were conducted within approximately 3 weeks. Duplicate and triplicate photochemical and electrochemical measurements were highly reproducible, indicating that there were no post-irradiation chemical alterations of the HS as detected by our methods.

Optical Properties and Absorbed Energy. Absorbance spectra were collected in 1 cm quartz cuvettes on a Cary 100 spectrophotometer (Varian) using 1 nm slits and phosphate buffer as a blank. Prior to measuring absorbance spectra, HS solutions were diluted in 5 mM phosphate buffer (pH 7.0) by a factor of three (SRFA and NAFA) or ten (ESHA) to ensure that measurements fell into the linear range of the instrument. Optical parameters, including the

E2/E3 ratio and specific UV absorbance at 280 nm (SUVA₂₈₀) were calculated from the measured spectra as detailed in the *Supporting Information*.

Absorption and lamp emission spectra were used to determine the energy absorbed between 300 and 500 nm during irradiation (details in *Supporting Information*). This wavelength range was chosen for its importance to HS photochemistry (20,34,43,47,51-56). The conclusions drawn in this study are based on relative changes and change little by setting the long wavelength cutoff to 400 or 450 nm.

Electrochemical Measurements. EDC and EAC values were quantified according to Aeschbacher *et al.* (44,45,57) in a glovebox under N₂ (O₂ < 0.1 ppm; 25 ± 1 °C, M. Braun Ltd., Germany). Anoxic buffer solutions were used as described previously (44,45,57). HS solutions (3.2 ml of each) from the photooxidation experiments were made anoxic by purging with argon for 20 min prior to transfer to the glovebox. Detailed methods are provided as *Supporting Information*.

Photochemical Experiments. Photooxidant quantum yields were determined using two merry-go-round reactors containing mercury vapor lamps having emission maxima at 365 nm (58-60). All quantum yields are therefore reported for excitation at 365 nm. Samples from photooxidation experiments were diluted prior to measuring the production of ¹O₂, H₂O₂, •OH, and triplet HS (³HS*). The transient species ¹O₂, •OH, and ³HS* were quantified using the probes furfuryl alcohol (FFA), terephthalate (TPA), and 2,4,6-trimethylphenol (TMP), respectively (36,59,61). Experimental details and the calculation of apparent quantum yields are provided as *Supporting Information*. Production rates of H₂O₂ were quantified using the Amplex Red assay (Invitrogen) (62). Analytical details and quantum yield calculations are provided as *Supporting Information*.

Results and Discussion

Optical Properties. Irradiation caused photobleaching in all the HS. Figure 1 shows the fraction of absorbance remaining and absolute changes in HS absorption coefficients after 59 h (absorption spectra provided as *Supporting Information*). Consistent with previous reports, larger absolute absorbance losses occurred at UV wavelengths, and higher percent losses occurred in the visible. These changes were accompanied by decreases in $SUVA_{280}$ and increases in E2/E3 (Fig. 2) (29,34,35,63). Large differences were observed between the soil-derived ESHA and the two aquatic FA in both the magnitude of the optical property changes and the type of changes observed. Specifically, SRFA and NAFA both showed extensive photobleaching (Fig. 1) and clear changes in $SUVA_{280}$ and E2/E3 that were approximately linear with the amount of energy absorbed (Fig. 2). In contrast, much less photobleaching occurred for ESHA even though it absorbed approximately twice the 300 to 500 nm energy (Fig. 1), and the changes in $SUVA_{280}$ and E2/E3 were much smaller and non-linear. These data suggest that ESHA was more resistant than the aquatic FAs to photooxidation. However, it is possible that this difference in resistance was exaggerated by inner-filtering in the ESHA solution. A substantially higher fraction of the energy absorbed by ESHA lay in the visible (ca. 90%) than for the aquatic FAs (ca. 70%), and visible irradiation is known to cause much less efficient photobleaching (34,35,64). Thus, the difference between the photobleaching efficiencies for ESHA and the aquatic FAs is probably not as large as implied by these data.

The difference in magnitude of the optical changes notwithstanding, all samples displayed loss of $SUVA_{280}$ and increases in E2/E3 with photobleaching. Both changes indicate loss of aromatic groups (65,66) and decreases in molecular weight (66,67). Indeed, decreases in molecular weight were observed by size-exclusion chromatography (*Supporting Information*)

189 accompanied by small (ca. 10%) losses of organic-C after 59 h of irradiation (*Supporting*
190 *Information*). The molecular weight dependence of E2/E3 is believed to derive from an
191 increased probability of electronic interactions between chromophores in larger DOM molecules.
192 Specifically, intramolecular charge transfer (CT) complexes involving electron-donating groups
193 (e.g., phenols) and electron-accepting groups (e.g., aromatic ketones and quinones) produces
194 broad, featureless absorbance in the near-UV and visible (i.e., above approximately 370 nm) (68-
195 70). Thus, observed increases in E2/E3 with irradiation suggest that CT complexes are being
196 destroyed, probably by both decreasing DOM molecular weight and photooxidation of donor
197 and/or acceptor moieties in DOM.

198 *Redox Properties and Relationships to Optical Properties.* In the CT model for DOM
199 optical properties, substituted phenols are suspected electron donors, and aromatic ketones and
200 possibly quinones are suspected acceptors (68-70). Phenols and quinones are also major
201 determinants of DOM electrochemical properties. For example, a diverse set of DOM showed a
202 strong correlation between EDC and phenol contents (44) (operationally defined as 2x the
203 titrated charge between pH 8 and 10 (71)). The EDC of DOM also varies with E_h and pH in
204 ways comparable to low molecular weight phenols (44). Finally, the EAC of DOM correlates
205 well with its % aromaticity (44), and DOM accepts electrons over a range of reduction potentials
206 consistent with quinones as major electron acceptors (45).

207 Figure 3 presents the changes in EDC and EAC with irradiation (values tabulated as
208 *Supporting Information*). The EDC values of all HS samples decreased monotonically with
209 increasing irradiation, with smaller decreases for ESHA that mirror the smaller changes observed
210 in its optical properties compared to the aquatic FAs. To our knowledge, this is the first direct
211 demonstration of DOM photooxidation as quantified by EDC loss. In comparison, all HS

212 samples showed small changes in EAC. This finding strongly suggests that there was no direct
213 relation between the changes in electron donating and accepting moieties, and, hence, that
214 photooxidation did not convert electron donating phenols and hydroquinones into electron
215 accepting quinone moieties. Instead, the fact that decreases in EDC were not accompanied by
216 similar increases in EAC suggests that photooxidation irreversibly destroyed phenolic moieties.
217 The reason for the small changes in EAC is unknown. They could reflect either a resistance to
218 oxidation by the relevant moieties or a pseudo-steady state resulting from their loss and
219 formation at approximately equal rates.

220 A comparison of Figs. 2 and 3 shows that the optical properties directly reflect the extent
221 of photooxidation and suggests that the optical properties depend on the amount and nature of
222 redox active moieties. To assess this, we reanalyzed the trends in SUVA₂₈₀ and E2/E3 as a
223 function of EDC and EAC (Figure 4). For the aquatic FAs, SUVA₂₈₀ displays a linear
224 relationship to EDC ($r^2 = 0.904$). For ESHA, there is no apparent relationship, possibly due to
225 the much smaller changes in EDC with irradiation. Stronger correlations of SUVA₂₈₀ with EDC
226 for the aquatic FAs than for soil HA are consistent with prior reports that aromatic-C and EDC
227 are well-correlated for diverse aquatic HS samples but not for different soil-derived HS (44).
228 Given that phenolic moieties constitute much more of the aromatic-C in the aquatic FAs than
229 ESHA (71,72) (*Supporting Information*), it appears likely that phenols are a major determinant
230 of both EDC and SUVA₂₈₀ in aquatic HS. In contrast, SUVA₂₈₀ appears to vary more with EAC
231 for ESHA (Fig. 4), which could imply that quinones are notable contributors to SUVA₂₈₀ in soil
232 HA. However, this conclusion is tempered by the small and irregular changes in EAC with
233 photooxidation.

To examine the relationship of E2/E3 to EDC and EAC, a larger data set was analyzed that included various untreated aquatic and soil HS (44) in addition to the photooxidized samples; missing E2/E3 ratios were measured. For aquatic HS, E2/E3 shows an inverse relationship to EDC, whereas for the soil HA these data are more scattered (Fig. 4). Furthermore, E2/E3 appears to be more sensitive to changes in EDC (steeper slope) for the photooxidized aquatic FAs than for untreated HS isolates. These observations suggest that (i) for aquatic HS, E2/E3 depends strongly on phenol content and (ii) that this dependence is pronounced in samples undergoing photooxidation. For soil HS, on the other hand, E2/E3 seems to be more dependent on EAC (Fig. 4), whereas this relationship is a bit more scattered for aquatic HS, and there is no obvious relationship for the photooxidized FAs. These differences suggest that quinones contribute more to CT absorbance in soil HS than in aquatic HS. Furthermore, in the aquatic FAs undergoing photooxidation, the extent of CT absorbance seems to be independent of quinones. This conclusion is consistent with recent evidence that quinones are not major determinants of CT absorbance in aquatic HS (46,70).

Photooxidant Quantum Yields. We further investigated the effect of irradiation on $^1\text{O}_2$, H_2O_2 , and $\cdot\text{OH}$ quantum yields (Φ), defined as the fraction of absorbed photons producing photooxidant. For $^3\text{HS}^*$, there is no method to quantify all of the $^3\text{HS}^*$ formed. Instead, a proxy for $\Phi_{^3\text{HS}^*}$ is used, the quantum yield coefficient, f_{TMP} (M^{-1}), which is the rate constant for TMP loss divided by the rate of light absorption (61). Although photochemical reaction rates are sometimes quantified as carbon-normalized rate constants (provided as *Supporting Information*), Φ is a more fundamental parameter with broader general applicability to photochemical modeling. Figure 5 shows how $\Phi_{^1\text{O}_2}$, $\Phi_{\text{H}_2\text{O}_2}$, Φ_{OH} and f_{TMP} vary with irradiation. For all HS, the quantum yields of H_2O_2 , $\cdot\text{OH}$, and $^3\text{HS}^*$ decreased, but, in stark contrast, $\Phi_{^1\text{O}_2}$ increased.

Attributing physical causes to these trends requires recognition that the quantum yields are “apparent” because they may be affected by a variety of secondary phenomena. For instance, $\Phi_{\text{H}_2\text{O}_2}$ is a function of the primary quantum yield of O_2^- and the relative rates of uncatalyzed versus HS-catalyzed O_2^- dismutation (36). Because uncatalyzed dismutation is apparently the dominant process during SRFA photolysis under conditions similar to those used here (73), decreases in $\Phi_{\text{H}_2\text{O}_2}$ likely reflect lower O_2^- production efficiencies rather than lower dismutation rates. It has recently been suggested that the excited state HS precursor to O_2^- is a long-lived charge-separated species created by electron transfer from singlet excited state donors to ground state acceptor moieties (74). The observed EDC loss is consistent with this model, as loss of donors would reduce the yield of charge-separated species and decrease $\Phi_{\text{H}_2\text{O}_2}$.

In the case of Φ_{OH} , the TPA probe detects both free $\cdot\text{OH}$ and other, lower energy hydroxylating species (59). Here, we do not distinguish between these hydroxylating species. However, control experiments were conducted with catalase to assess the contribution of H_2O_2 -dependent, Fenton-like hydroxylation (59). Irradiation did not significantly alter the fraction of hydroxylation occurring through H_2O_2 -dependent pathways, which was approximately 50% for ESHA and 20% for SRFA, in good agreement with a previous report (59). For NAFA, there was essentially no TPA hydroxylation via H_2O_2 . Thus, only a fraction of the decrease in Φ_{OH} can be ascribed to the decrease in $\Phi_{\text{H}_2\text{O}_2}$. The remainder must be due to lower quantum yields of excited state oxidants, which are of unknown character, because the mechanism of $\cdot\text{OH}$ production by DOM is not established.

The parameter used to assess $^3\text{HS}^*$ formation, f_{TMP} , depends on both the primary quantum yield of $^3\text{HS}^*$ and the rate constant for reaction between $^3\text{HS}^*$ and TMP (61). Notably, HS do not inhibit TMP oxidation (58). Decreases in f_{TMP} thus reflect either a general decrease in $^3\text{HS}^*$

precursor chromophores or a decrease in a specific $^3\text{HS}^*$ pool that reacts rapidly with TMP. In either case, the observed decreases in f_{TMP} indicate that photooxidant production efficiency decreases with irradiation, in agreement with the Φ_{OH} results. For TMP oxidation, the $^3\text{HS}^*$ precursors are believed to be mainly aromatic ketones and possibly quinones (46,61). The present data provide divergent evidence for the role of quinones. For instance, the aquatic FAs have much lower EAC and f_{TMP} than ESHA, consistent with excited state quinones as oxidants of TMP. However, this conclusion does not seem to be compatible with the fact that decreases in f_{TMP} were not paralleled by comparable decreases in EAC.

Distinct from the other quantum yields, $\Phi_{1\text{O}_2}$ increased with irradiation. Note that the FFA probe detects $^1\text{O}_2$ in the bulk aqueous phase that has escaped the HS microenvironment without being quenched therein (75). It is generally accepted that $^1\text{O}_2$ is produced by energy transfer from $^3\text{HS}^*$ to O_2 . Reports by Halladja *et al.* (76) and Sharpless (47) indicate that a high degree of overlap exists between the $^3\text{HS}^*$ pools that produce $^1\text{O}_2$ and those that oxidize TMP. If true, a simple way to reconcile the increases in $\Phi_{1\text{O}_2}$ with the decreases in f_{TMP} is to hypothesize that irradiation decreases the efficiency of $^1\text{O}_2$ quenching by HS. Thus, even if the yield of $^3\text{HS}^*$ decreases, higher $^1\text{O}_2$ yields could be observed if $^1\text{O}_2$ is less effectively quenched within the DOM microenvironment. The loss of EDC is consistent with this hypothesis because quenching of $^1\text{O}_2$ by HS probably occurs by an electron transfer mechanism (77), which is expected to become less effective as electron donors in HS are destroyed. Also consistent with this view is a recent report that wastewater DOM $\Phi_{1\text{O}_2}$ increases with chemical oxidation by both ozone and chlorine, which destroy electron rich groups selectively and non-selectively, respectively (41). An alternative explanation for the increases in $\Phi_{1\text{O}_2}$ is that there may be two classes of $^1\text{O}_2$ sensitizer (e.g., aromatic ketones and quinones), and that only one of these (Class 1) strongly

determines HS optical properties. The destruction of Class 1 sensitizers would decrease absorbance, but the other class of sensitizer would continue producing $^1\text{O}_2$. Hence, the results can also be accommodated by a model in which aromatic ketones are Class 1 sensitizers, and quinones are the other Class. This is consistent with negligible EAC loss accompanied by large changes in E2/E3 in the aquatic FAs, where the loss of aromatic ketones would be expected to greatly alter the optical properties (see preceding section) (46,70). The hypothesis is also consistent with increasing $\Phi_{1\text{O}_2}$ in the absence of large E2/E3 changes for ESHA; here, quinones may be contributing more to both the photochemical and optical properties (see preceding section) as other sensitizing chromophores are destroyed.

Relationship of $\Phi_{\text{H}_2\text{O}_2}$ and $\Phi_{1\text{O}_2}$ to Optical and Redox Properties. Previous reports have demonstrated correlations of E2/E3 with $\Phi_{\text{H}_2\text{O}_2}$ and $\Phi_{1\text{O}_2}$ (36,37). Sharpless and co-workers have argued that these originate from the influence of CT interactions on both the optical properties and photochemistry of DOM (36). Because photooxidation is an important natural DOM transformation process, we explored whether our results conform to the previously reported correlations. We further investigated relationships between photochemical and electrochemical properties. Figure 6 shows $\Phi_{1\text{O}_2}$ and $\Phi_{\text{H}_2\text{O}_2}$ as a function of both E2/E3 and EDC for samples undergoing photooxidation. Related plots involving f_{TMP} and $\Phi_{\text{H}_2\text{O}_2}$ and EAC are provided as *Supporting Information*. We did not construct plots using SUVA_{280} , as it correlates inversely and strongly with E2/E3 (*Supporting Information*). Such plots would simply display the reverse of the trends in Figure 6. Although the directions of the trends were the same for all samples, $\Phi_{\text{H}_2\text{O}_2}$ and $\Phi_{1\text{O}_2}$ vary much more with both E2/E3 and EDC for ESHA than for the aquatic FAs.

Figure 6 also presents the results of Dalrymple *et al.*, who studied HS and DOM isolates (36), and Peterson *et al.*, who studied whole water from Lake Superior and its tributaries (37). Peterson *et al.*'s results are shown as the reported linear trend because the data include many samples with E2/E3 values well above the range used in Figure 6. For the aquatic FAs undergoing photooxidation, the directions of the trends in $\Phi_{H_2O_2}$ and Φ_{1O_2} with E2/E3 agree with previous reports (36,37). The $\Phi_{H_2O_2}$ results display good quantitative agreement with those of Dalrymple *et al.* (36), suggesting that E2/E3 may be a robust predictor of $\Phi_{H_2O_2}$. However, Φ_{1O_2} is less sensitive to changes in E2/E3 for the photooxidized FAs than for untreated DOM isolates. Notably, the relationship between Φ_{1O_2} and E2/E3 for photooxidized FAs resembles that of the Lake Superior samples much more than that of the untreated DOM. This suggests that photobleaching is a major control on DOM optical properties and photochemistry in Lake Superior. Furthermore, it indicates that DOM photooxidation or other dominant DOM degradation processes in particular ecosystems may lead to watershed-specific correlations between optical and photochemical properties.

With EDC, a weak decreasing trend in Φ_{1O_2} is observed, while $\Phi_{H_2O_2}$ increases sharply, albeit with different slopes for aquatic HS and soil HS (Fig. 6). The trends can be explained in terms of photophysical concepts expounded previously (36,47,74). For example, the decrease in Φ_{1O_2} with EDC could reflect lower $^3HS^*$ yields in samples where higher concentrations of electron donating groups engage electron accepting photosensitizers in CT complexes, thus producing absorbance that does not lead to $^3HS^*$ (36,47). Conversely, the increase in $\Phi_{H_2O_2}$ with EDC could result from increased formation of charge-separated excited-state precursors to H_2O_2 (74) as the content of electron donors increases. As shown in the *Supporting Information*, Φ_{1O_2} for the photooxidized FAs and several IHSS aquatic HS and DOM isolates follow similar inverse

relationships to both EDC and EAC, suggesting that DOM with higher concentrations of redox active moieties sensitize $^1\text{O}_2$ production less efficiently. This point is also illustrated by plotting $\Phi_{1\text{O}_2}$ versus the total redox activity (EDC + EAC) for all samples in this study plus others for which $\Phi_{1\text{O}_2}$, EDC, and EAC are available (*Supporting Information*).

Environmental Implications. Aquatic HS have much higher EDC than soil HS, while the opposite is true for EAC (44). The present results show that irradiation destroys EDC but alters EAC very little. The lack of EAC creation, even while EDC is destroyed, argues against photochemical oxidation of donor groups to acceptor groups. Rather, the accumulated data point to irreversible oxidation, the target of which may be phenols. Additionally, the photochemical results suggest that aromatic ketones and other possible $^3\text{DOM}^*$ precursors such as flavones and chromones are rapidly destroyed by photooxidation.

These results predict a decrease in all photooxidant quantum yields except $^1\text{O}_2$ in natural systems where DOM undergoes photooxidation. The direct implication of this finding is that constant quantum yields for HS-derived photooxidants cannot be assumed over the course of days of solar exposure. Based on the energy absorbed in our photooxidation experiments, we estimate that the changes observed here would occur with approximately 240 h of summer solar noon irradiation at 41°N in the upper first cm of a typical inland water (5 mg OC of aquatic DOM from terrestrial sources). However, this estimate is confounded some by uncertainties, such as the extent to which inner-filtering altered the observed photobleaching efficiencies in these experiments and the extent to which storage of our solutions at high concentration for 3 d after irradiation may have fostered intermolecular redox reactions that would not be observed in natural waters. Nonetheless, the contrast between the photochemical trends for photooxidized and untreated HS and DOM (Fig. 6) suggests that variability in photochemical properties of natural

waters may arise from multiple processes – mixing of different DOM sources, or photooxidation of a single DOM source – each of which can uniquely alter the optical-photochemical correlations. It is also apparent that compositional differences between aquatic and soil HS lead to very different controls on the optical behavior and hence very different correlations between the optical and photochemical properties. Further efforts to relate the optical and photochemical properties to DOM structure will be needed to provide a sound basis for understanding DOM source-dependent differences in behavior.

Acknowledgements

The authors acknowledge Annika Linkhorst for assistance with the spectroscopic measurements, Silvio Canonica and Urs von Gunten for providing facilities and equipment at Eawag, Neil Blough for helpful discussions, and three anonymous reviewers for their insights and comments.

Supporting Information Available

Chemicals used, absorption spectra; optical properties; calculations of absorbed energy; electrochemistry details; photochemistry experimental details and calculations; TOC method and results; SEC-OCD results; phenol and aromatic C content of HS; E2/E3 and SUVA₂₈₀ relationship to aromaticity; tabulated EDC and EAC; carbon-normalized rates and rate constants for photochemical experiments; f_{TMP} and Φ_{OH} versus E2/E3 and EDC; photooxidant quantum yields versus EAC; correlation between E2/E3 and SUVA₂₈₀; Φ_{IO_2} versus EDC and EAC and versus (EDC + EAC)

1. Thurman, E. M. *Organic Geochemistry of Natural Waters*; Martinus Nijhoff/Junk: Netherlands, 1985.
2. Piccolo, A. The supramolecular structure of soil humic substances: a novel understanding of humus chemistry and implications in soil science. In *Advances in Agronomy (book series)*; Sparks, D., Ed.; Academic Press, 2002; Vol. 75.
3. Lovley, D. R.; Coates, J. D.; Blunt-Harris, E. L.; Phillips, E. J. P.; Woodward, J. C. Humic substances as electron acceptors for microbial respiration. *Nature* 1996 **1996**, 382, 445-448.
4. Lu, Y.; Pignatello, J. J. History-dependent sorption in humic acids and a lignite in the context of a polymer model for natural organic matter. *Environ. Sci. Technol.* **2004**, 38, 5853-5862.
5. Christl, I.; Milne, C. J.; Kinniburgh, D. G.; Kretzschmar, R. Relating ion binding by fulvic and humic acids to chemical composition and molecular size. 2. Metal binding. *Environ. Sci. Technol.* **2001**, 35, 2512-2517.
6. Brinkmann, T.; Sartorius, D.; Frimmel, F. H. Photobleaching of humic rich dissolved organic matter. *Aquat. Sci.* **2003**, 65, 415-424.
7. Blough, N. V.; Zepp, R. G. Reactive oxygen species in natural waters. In *In Active Oxygen in Chemistry*; Foote, C. S., Valentine, J. S., Greenberg, A., Liebman, J. F., Eds.; Chapman & Hall, 1995.
8. Richard, C.; Canonica, S. Aquatic phototransformation of organic contaminants induced by coloured dissolved organic matter. In *Handbook of Environmental Chemistry, vol. 2, Part M*; Hutzinger, O., Ed.; Springer-Verlag: Berlin, 2005; p 299-323.
9. Canonica, S. Oxidation of aquatic organic contaminants induced by excited triplet states. *Chimia* **2007**, 61, 641-644.
10. Sulzberger, B. Effects of light on the biological availability of trace metals. In *Marine Chemistry*; Gianguzza, A., Pelizzetti, E., Sammartano, S., Eds.; Kluwer Academic Publishers, 1997.
11. Voelker, B. M.; Morel, F. M. M.; Sulzberger, B. Iron redox cycling in surface waters: Effects of humic substances and light. *Environ. Sci. Technol.* **1997**, 31, 1004-1011.
12. Gabarell, M.; Chin, Y.-P.; Hug, S. J.; Sulzberger, B. Role of dissolved organic matter composition on the photoreduction of Cr(VI) to Cr(III) in the presence of iron. *Environ. Sci. Technol.* **2003**, 37, 4403-4409.
13. Guerard, J. J.; Chin, Y.-P.; Mash, H.; Hadad, C. M. Photochemical fate of sulfadimethoxine in aquaculture waters. *Environ. Sci. Technol.* **2009**, 43, 8587-8592.
14. Latch, D. E.; Stender, B. L.; Arnold, W. A.; McNeill, K. Photochemical fate of pharmaceuticals in the

- environment: cimetidine and ranitidine. *Environ. Sci. Technol.* **2003**, *37*, 3342-3350.
15. Gerecke, A. C.; Canonica, S.; Müller, S.; Sharer, M.; Schwarzenbach, R. P. Quantification of dissolved natural organic matter (DOM) mediated phototransformation of phenylurea herbicides in lakes. *Environ. Sci. Technol.* **2001**, *35*, 3915-3923.
 16. Romero, O. C.; Straub, A. P.; Kohn, T.; Nguyen, T. H. Role of temperature and Suwannee River Natural Organic Matter on inactivation kinetics of rotavirus and bacteriophage MS2 by Solar Irradiation. *Environ. Sci. Technol.* **2011**, *45*, 10385-10393.
 17. Wetzel, R. G.; Hatcher, P. G.; Bianchi, T. S. Natural photolysis by ultraviolet irradiance of recalcitrant dissolved organic matter to simple substrates for rapid bacterial metabolism. *Limnol. Oceanogr.* **1995**, *40*, 1369-1380.
 18. Miller, W. L.; Zepp, R. G. Photochemical production of dissolved inorganic carbon from terrestrial organic matter: significance to the oceanic organic carbon cycle. *Geophys. Res. Lett.* **1995**, *22*, 417-420.
 19. Pullin, M. J.; Bertilsson, S.; Goldstone, J. V.; Voelker, B. M. Effects of sunlight and hydroxyl radical on dissolved organic matter: bacterial growth efficiency and production of carboxylic acids and other substrates. *Limnol. Oceanogr.* **2004**, *49*, 2011-2022.
 20. White, E. M.; Kieber, D. J.; Sherrard, J.; Miller, W. L.; Mopper, K. Carbon dioxide and carbon monoxide photoproduction quantum yields in the Delaware Estuary. *Mar. Chem.* **2010**, *118*, 11-21.
 21. de Bruyn, W. J.; Clark, C. D.; Pagel, L.; Takehara, C. Photochemical production of formaldehyde, acetaldehyde and acetone from chromophoric dissolved organic matter in coastal waters. *J. Photochem. Photobiol. A: Chem.* **2001**, *226*, 16-22.
 22. Osburn, C. L.; Wigdahl, C. R.; Fritz, S. C.; Saros, J. E. Dissolved organic matter composition and photoreactivity in prairie lakes of the U.S. Great Plains. *Limnol. Oceanogr.* **2011**, *56*, 2371-2390.
 23. Wang, W.; Johnson, C. G.; Takeda, K.; Zafiriou, O. C. Measuring the photochemical production of carbon dioxide from marine dissolved organic matter by pool isotope exchange. *Environ. Sci. Technol.* **2009**, *43*, 8604-8609.
 24. Opsahl, S.; Benner, R. Photochemical reactivity of dissolved lignin in river and ocean waters. *Limnol. Oceanogr.* **1998**, *43*, 1297-1304.
 25. Scully, N. M.; Maie, N.; Dailey, S. K.; Boyer, J. N.; Jones, R. D.; Jaffé, R. Early diagenesis of plant-derived dissolved organic matter along a wetland, mangrove, estuary ecotone. *Limnol. Oceanogr.* **2004**, *49*, 1667-1678.
 26. Spencer, R. G. M.; Stubbins, A.; Hernes, P. J.; Baker, A.; Mopper, K.; Aufdenkampe, A. K.; Dyda, R. Y.; Mwamba, V. L.; Mangangu, A. M.; Wabakanganzi, J. N.; Six, J. Photochemical degradation of

- dissolved organic matter and dissolved lignin phenols from the Congo River. *J. Geophys. Res.* **2009**, *114*, G03010, doi:10.1029/2009JG000968.
27. Stubbins, A.; Spencer, R. G. M.; Chen, H.; Hatcher, P. G.; Mopper, K.; Hernes, P. J.; Mwamba, V. L.; Mangangu, A. M.; Wabakanghanzi, J. N.; Six, J. Illuminated darkness: molecular signatures of Congo River dissolved organic matter and its photochemical alteration as revealed by ultrahigh precision mass spectrometry. *Limnol. Oceanogr.* **2010**, *55*, 1467-1477.
 28. Thorn, K. A.; Younger, S. J.; Cox, L. G. Order of functionality loss during photodegradation of aquatic humic substances. *J. Environ. Qual.* **2010**, *39*, 1416-1428.
 29. Helms, J. R.; Stubbins, A.; Ritchie, J. D.; Minor, E. C.; Kieber, D. J.; Mopper, K. Absorption spectral slopes and slope ratios as indicators of molecular weight, source, and photobleaching of chromophoric dissolved organic matter. *Limnol. Oceanogr.* **2008**, *53*, 955-969.
 30. Hernes, P. J.; Bergamaschi, B. A.; Eckard, R. S.; Spencer, R. M. Fluorescence-based proxies for lignin in freshwater dissolved organic matter. *J. Geophys. Res.* **2009**, *114*, G00F03, doi:10.1029/2009JG000938.
 31. Dalzell, B. J.; Minor, E. C.; Mopper, K. M. Photodegradation of estuarine dissolved organic matter: a multi-method assessment of DOM transformation. *Org. Geochem.* **2009**, *40*, 243-257.
 32. Kouassi, A. M.; Zika, R. G. Light-induced alteration of the photophysical properties of dissolved organic matter in seawater. Part I. Photoreversible properties of natural water fluorescence. *Neth. J. Sea Res.* **1990**, *27*, 25-32.
 33. Lou, T.; Xie, H. Photochemical alteration of the molecular weight of dissolved organic matter. *Chemosphere* **2006**, *65*, 2333-2342.
 34. Del Vecchio, R.; Blough, N. V. Photobleaching of chromophoric dissolved organic matter in natural waters: kinetics and modeling. *Mar. Chem.* **2002**, *78*, 231-253.
 35. Tzortziou, M.; Osburn, C. L.; Neale, P. J. Photobleaching of dissolved organic material from a tidal marsh-estuarine system of the Chesapeake Bay. *Photochem. Photobiol.* **2007**, *83*, 782-792.
 36. Dalrymple, R. M.; Carfagno, A. K.; Sharpless, C. M. Correlations between dissolved organic matter optical properties and quantum yields of singlet oxygen and hydrogen peroxide. *Environ. Sci. Technol.* **2010**, *44*, 5824-5829.
 37. Peterson, B.; McNally, A. M.; Cory, R. M.; Thoemke, J. D.; Cotner, J. B.; McNeill, K. Spatial and temporal distribution of singlet oxygen in Lake Superior. *Environ. Sci. Technol.* **2012**, *46*, 7222-7229.
 38. Zhang, Y.; Xie, H.; Chen, G. Factors affecting the efficiency of carbon monoxide photoproduction in the St. Lawrence estuarine system (Canada). *Environ. Sci. Technol.* **2006**, *40*, 7771-7777.

39. Xie, H.; Bélanger, S.; Demers, S.; Vincent, W. F.; Papakyriakou, T. N. Photobiogeochemical cycling of carbon monoxide in the southeastern Beaufort Sea in spring and autumn. *Limnol. Oceanogr.* **2009**, *54*, 234–249.
40. Stubbins, A.; Law, C. S.; Uher, G.; Upstill-Goddard, R. C. Carbon monoxide apparent quantum yields and photoproduction in the Tyne estuary. *Biogeosci.* **2011**, *8*, 703–713.
41. Mostafa, S.; Rosario-Ortiz, F. L. Singlet oxygen formation from wastewater organic matter. *Environ. Sci. Technol.* **2013**, *47*, 8179–8186.
42. Cavani, L.; Halladja, S.; Ter Halle, A.; Guyot, G.; Corrado, G.; Ciavatta, C.; Boulkamh, A.; Richard, C. Relationship between photosensitizing and emission properties of peat humic acid fractions obtained by tangential ultrafiltration. *Environ. Sci. Tech.* **2009**, *43*, 4348–4354.
43. Andrews, S. S.; Caron, S.; Zafiriou, O. C. Photochemical oxygen consumption in marine waters: A major sink for colored dissolved organic matter? *Limnol. Oceanogr.* **2000**, *45*, 267–277.
44. Aeschbacher, M.; Graf, C.; Schwarzenbach, R. P.; Sander, M. Antioxidant properties of humic substances. *Environ. Sci. Technol.* **2012**, *46*, 4916–4925.
45. Aeschbacher, M.; Vergari, D.; Schwarzenbach, R. P.; Sander, M. Electrochemical analysis of proton and electron transfer equilibria of the reducible moieties in humic acids. *Environ. Sci. Technol.* **2011**, *44*, 87–93.
46. Golanoski, K.; Fang, S.; Del Vecchio, R.; Blough, N. V. Investigating the mechanism of phenol photooxidation by humic substances. *Environ. Sci. Technol.* **2012**, *46*, 3912–3920.
47. Sharpless, C. M. Lifetimes of triplet dissolved natural organic matter (DOM) and the effect of NaBH₄ reduction on singlet oxygen quantum yields: Implications for DOM photophysics. *Environ. Sci. Technol.* **2012**, *46*, 4466–4473.
48. Vaughan, P. P.; Blough, N. V. Photochemical formation of hydroxyl radical by constituents of natural waters. *Environ. Sci. Technol.* **1998**, *32*, 2947–2953.
49. Gan, D.; Jia, M.; Vaughan, P. P.; Falvey, D. E.; Blough, N. V. Aqueous photochemistry of methylbenzoquinone. *J. Phys. Chem. A* **2008**, *112*, 2803–2812.
50. Dulin, D.; Mill, T. Development and evaluation of sunlight actinometers. *Environ. Sci. Technol.* **1982**, *16*, 815–820.
51. Cooper, W. J.; Zika, R. G. Photochemical formation of hydrogen peroxide in surface and ground waters exposed to sunlight. *Science* **1983**, *220*, 711–712.
52. Haag, W. R.; Hoigné, J.; Gassman, E.; Braun, A. M. Singlet oxygen in surface waters – part II: quantum yields of its production by some natural humic materials as a function of wavelength.

Chemosphere **1984**, *13*, 641-650.

53. Johannessen, S. C.; Miller, W. L. Quantum yield for the photochemical production of dissolved inorganic carbon in seawater. *Mar. Chem.* **2001**, *76*, 271-283.
54. O'Sullivan, D. W.; Neale, P. J.; Coffin, R. B.; Boyd, T. J.; Osburn, C. L. Photochemical production of hydrogen peroxide and methylhydroperoxide in coastal waters. *Mar. Chem.* **2005**, *97*, 14-33.
55. Osburn, C. L.; Retamal, L.; Vincent, W. F. Photoreactivity of chromophoric dissolved organic matter transported by the Mackenzie River to the Beaufort Sea. *Mar. Chem.* **2009**, *115*, 10-20.
56. Paul, A.; Hackbarth, S.; Vogt, R. D.; Röder, B.; Burnison, B. K.; Steinburg, C. E. W. Photogeneration of singlet oxygen by humic substances: comparison of humic substances of aquatic and terrestrial origin. *Photochem. Photobiol. Sci.* **2004**, *3*, 273-280.
57. Aeschbacher, M.; Sander, M.; Schwarzenbach, R. P. Novel electrochemical approach to assess the redox properties of humic substances. *Environ. Sci. Technol.* **2010**, *44*, 87-93.
58. Wenk, J.; von Gunten, U.; Canonica, S. Effect of dissolved organic matter on the transformation of contaminants induced by excited triplet states and the hydroxyl radical. *Environ. Sci. Technol.* **2011**, *45*, 1334-1340.
59. Page, S. E.; Arnold, W. A.; McNeill, K. Assessing the contribution of free hydroxyl radical in organic matter-sensitized photohydroxylation reactions. *Environ. Sci. Technol.* **2011**, *45*, 2818-2825.
60. Wenk, J.; Canonica, S. Phenolic antioxidants inhibit the triplet-induced transformation of anilines and sulfonamide antibiotics in aqueous solution. *Environ. Sci. Technol.* **2012**, *46*, 5455-5462.
61. Canonica, S.; Jans, U.; Stemmler, K.; Hoigné, J. Transformation kinetics of phenols in water: photosensitization by dissolved natural organic material and aromatic ketones. *Environ. Sci. Technol.* **1995**, *29*, 1822-1831.
62. Zhou, M.; Diwu, Z.; Panchuk-Voloshina, N.; Haugland, R. P. A stable nonfluorescent derivative of resorufin for the fluorometric determination of trace hydrogen peroxide: applications in detecting the activity of phagocyte NADPH oxidase and other oxidases. *Anal Biochem.* **1997**, *253*, 162-168.
63. Helms, J. R.; Stubbins, A.; Perdue, E. M.; Green, N. W.; Chen, H.; Mopper, K. Photochemical bleaching of oceanic dissolved organic matter and its effect on absorption spectral slope and fluorescence. *Mar. Chem.* **2013**, *155*, 81-91.
64. Goldstone, J. V.; Del Vecchio, R.; Blough, N. V.; Voelker, B. M. A multicomponent model of chromophoric dissolved organic matter photobleaching. *Photochem. Photobiol.* **2004**, *80*, 52-60.
65. Weishaar, J. L.; Aiken, G. R.; Bergamaschi, B. A.; Fram, M. S.; Fujii, R.; Mopper, K. Evaluation of specific ultraviolet absorption as an indicator of the chemical composition and reactivity of dissolved

- organic carbon. *Environ. Sci. Technol.* **2003**, *37*, 4702-4708.
66. Peuravuori, J.; Pihlaja, K. Molecular size distribution and spectroscopic properties of aquatic humic substances. *Anal. Chim. Acta* **1997**, *337*, 133-149.
 67. Peuravuori, J.; Pihlaja, K. Preliminary study of lake dissolved organic matter in light of nanoscale supramolecular assembly. *Environ. Sci. Technol.* **2004**, *38*, 5958-5967.
 68. Korshin, G. V.; Li, C.-W.; Benjamin, M. M. Monitoring the properties of natural organic matter through UV spectroscopy: a consistent theory. *Wat. Res.* **1997**, *31*, 1787-1795.
 69. Del Vecchio, R.; Blough, N. V. On the origin of the optical properties of humic substances. *Environ. Sci. Technol.* **2004**, *38*, 3885-3891.
 70. Ma, J.; Del Vecchio, R.; Golanoski, K. S.; Boyle, E. S.; Blough, N. V. Optical properties of humic substances and CDOM: effects of borohydride reduction. *Environ. Sci. Technol.* **2010**, *44*, 5395-5402.
 71. Ritchie, J. D.; Perdue, E. M. Proton-binding study of standard and reference fulvic acids, humic acids, and natural organic matter. *Geochim. Cosmochim. Acta* **2003**, *67*, 85-96.
 72. Thorn, K. A.; Folan, D. W.; MacCarthy, P. *Characterization of the International Humic Substances Society standard and reference fulvic and humic acids by solution state carbon-13 (¹³C) and hydrogen-1 (¹H) nuclear magnetic resonance spectrometry*; Water-Resources Investigations Report 89-4196; U.S. Geological Survey: Denver, 1989.
 73. Garg, S.; Rose, A. L.; Waite, T. D. Photochemical production of superoxide and hydrogen peroxide from natural organic matter. *Geochim. Cosmochim. Acta* **2011**, *75*, 4310-4320.
 74. Zhang, Y.; Del Vecchio, R.; Blough, N. V. Investigating the mechanism of hydrogen peroxide photoproduction by humic substances. *Environ. Sci. Technol.* **2012**, *46*, 11836-11843.
 75. Latch, D. E.; McNeill, K. Microheterogeneity of singlet oxygen distributions in irradiated humic acid solutions. *Science* **2006**, *311*, 1743-1747.
 76. Halladja, S.; ter Halle, A.; Aguer, J.-P.; Boulkamh, A.; Richard, C. Inhibition of humic substances mediated photooxygenation of furfuryl alcohol by 2,4,6-trimethylphenol. Evidence for reactivity of the phenol with humic triplet excited states. *Environ. Sci. Technol.* **2007**, *41*, 6066-6073.
 77. Foote, C. S.; Clennan, E. L. Properties and reactions of singlet oxygen. In *Active Oxygen in Chemistry*; Foote, C. S., Valentine, J. S., Greenburg, A., Liebman, J. F., Eds.; Blackie Academic and Professional: Glasgow, 1995.

Figure Captions

Figure 1: Change in absorbance with irradiation time: (a) $f_{A,59h}$, fraction of absorbance remaining at 59 h; (b) Δa_{59h} , change in absorbance at 59 h (base-10 absorption coefficient).

Figure 2: Changes in (a) $SUVA_{280}$ ($L\ mg^{-1}\ m^{-1}$) and (b) E2/E3 versus energy absorbed from 300 to 500 nm: (●) SRFA; (◇) NAFA; (▲) ESHA.

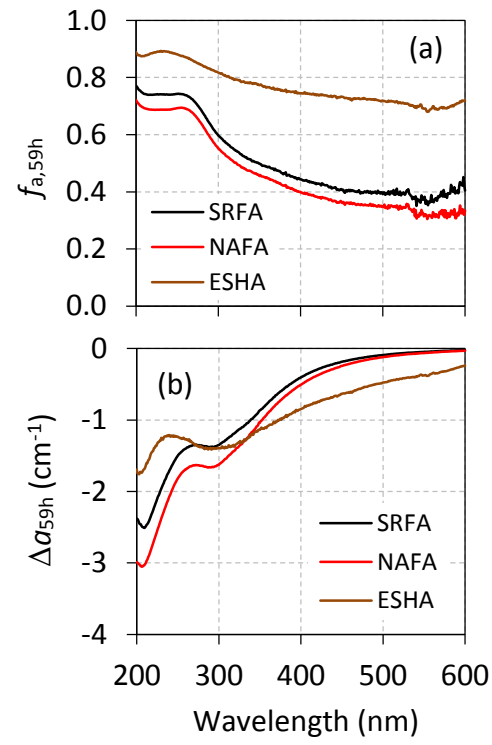
Figure 3: Change in EDC and EAC with irradiation time. Samples taken at 0, 11, 35, and 59 h.

Figure 4: $SUVA_{280}$ ($L\ mg^{-1}\ m^{-1}$) (top) and E2/E3 (bottom) versus EDC (pH 7, 0.73 V) and EAC (pH 7, -0.49 V): (●) SRFA; (◇) NAFA; (▲) ESHA. For E2/E3, data are also included for IHSS isolates: aquatic (x); soil (○) (redox data from Aeschbacher *et al.* (44)).

Figure 5: Changes in photooxidant quantum yields with irradiation time. Error bars represent standard deviation of duplicate or triplicate measurements. (●) SRFA; (◇) NAFA; (▲) ESHA.

Figure 6: Quantum yields of 1O_2 and H_2O_2 versus E2/E3 and EDC. (●) SRFA; (◇) NAFA; (▲) ESHA; (■) data from Dalrymple *et al.* (36); (---) trend reported by Peterson *et al.* (37).

Figure 1



426

Figure 2

427

428

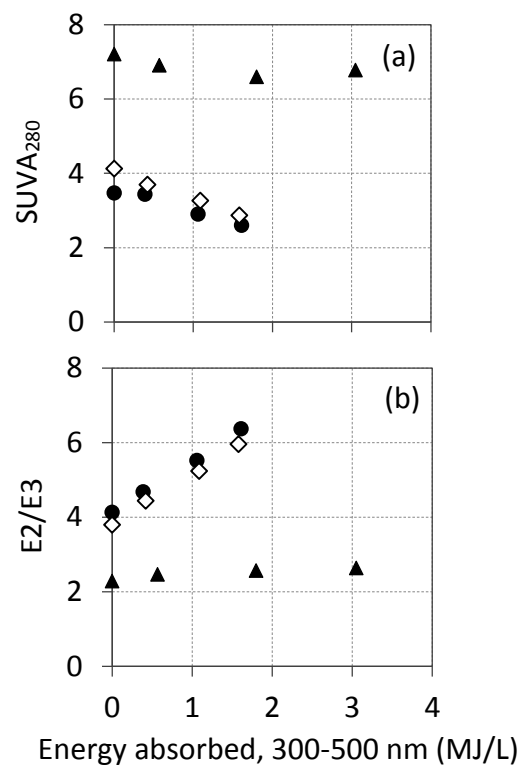


Figure 3

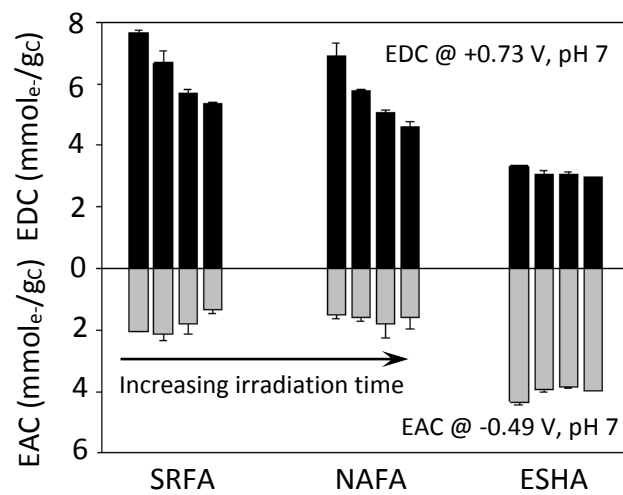


Figure 4

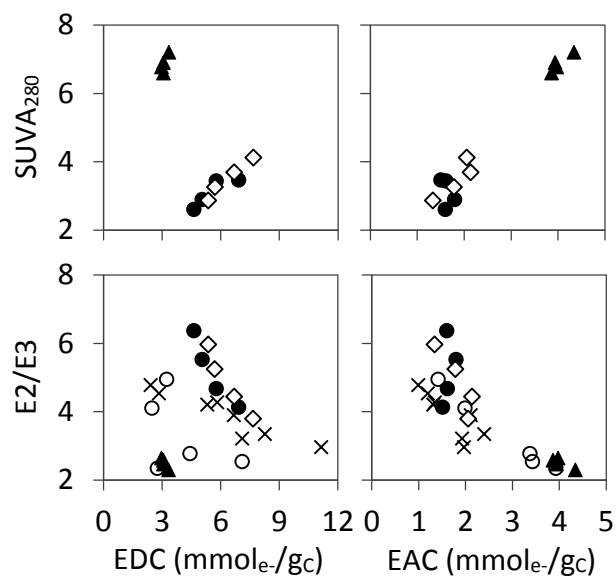


Figure 5

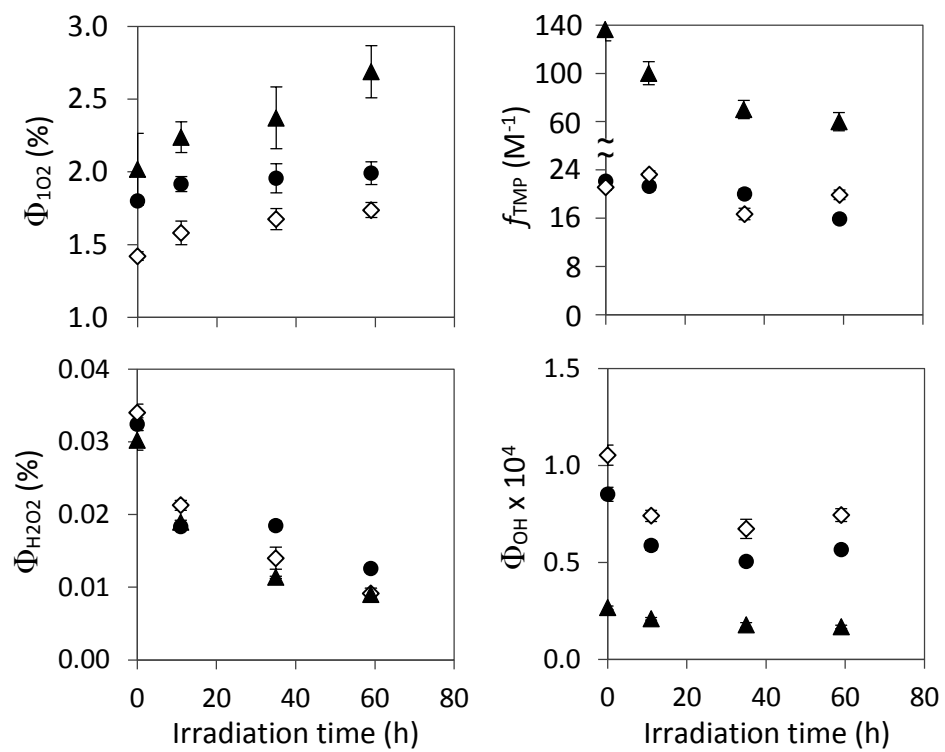
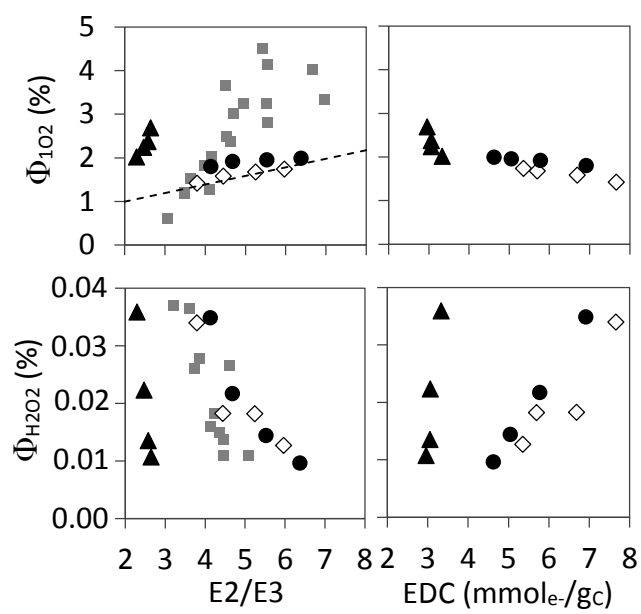


Figure 6



462

463

TOC ART

464

465

466

467

